

# Anisotropy in the Interaction of Ultracold Dysprosium

Svetlana Kotochigova\* and Alexander Petrov†

*Department of Physics, Temple University, Philadelphia, PA 19122-6082, USA*

The nature of the interaction between ultracold atoms with a large orbital and spin angular momentum has attracted considerable attention. It was suggested that such interactions can lead to the realization of exotic states of highly correlated matter. Here, we report on a theoretical study of the competing anisotropic dispersion, magnetic dipole-dipole, and electric quadrupole-quadrupole forces between two dysprosium atoms. Each dysprosium atom has an orbital angular momentum  $L = 6$  and magnetic moment  $\mu = 10\mu_B$ . We show that the dispersion coefficients of the ground state adiabatic potentials lie between 1865 a.u. and 1890 a.u., creating a non-negligible anisotropy with a spread of 25 a.u. and that the electric quadrupole-quadrupole interaction is weak compared to the other interactions. We also find that for interatomic separations  $R < 50 a_0$  both the anisotropic dispersion and magnetic dipole-dipole potential are larger than the atomic Zeeman splittings for external magnetic fields of order 10 G to 100 G. At these separations spin exchange can occur. We finish by describing two scattering models for inelastic spin exchange. A universal scattering theory is used to model loss due to the anisotropy in the dispersion and a distorted-wave-Born theory is used to model losses from the magnetic dipole-dipole interaction for the  $^{164}\text{Dy}$  isotope. These models find loss rates that are the same order of magnitude as the experimental value.

## I. INTRODUCTION

In recent years significant effort has been devoted to the characterization of the interactions with submerged-shell 3d-transition-metal and 4f-rare-earth atoms [1–8]. These atoms have an electronic configuration with an unfilled inner shell shielded by a closed outer shell. They also tend to have a large magnetic moment due to a large number of unpaired electrons, which presents opportunities to explore the effect of anisotropic magnetic dipole-dipole interactions between them. Long-range dipolar interactions create conditions for realizing novel quantum states of highly correlated ultracold atomic matter [7, 9]. This physics complements that proposed with ultracold polar molecules, another system in which exotic quantum phases are predicted [10–13]. Here, dipole-dipole forces originate from a non-zero electric dipole moment. Unlike for magnetic atoms, however, the electric dipole moment must be induced by an external electric field.

Submerged shell atoms are expected to have significantly suppressed inelastic, energy-releasing spin-exchange collisions because of shielding caused by the closed outer-shell electrons. This effect was first predicted and demonstrated for collisions between submerged-shell atoms with helium [2–4, 14]. The suppression of inelastic loss with the He atom indicates that there is no collisional anisotropy. The spherically symmetric He atom can not take up angular momentum from the submerged-shell atom.

Recent measurements of the spin-exchange rates between two submerged-shell atoms, however, have seen

no suppression and, in fact, the rate coefficients are of the same order of magnitude as for non-submerged shell atoms [6, 8, 15]. A possible explanation for this phenomena, given in Ref. [8], is that most submerged-shell atoms have a non-zero orbital electron angular momentum  $L$ . This leads a non-zero electrostatic quadrupole moment and anisotropic quadrupole-quadrupole interaction that, in principle, can cause substantial losses.

In this paper we propose and discuss another mechanism that leads to losses. We will show that the large loss rate of order  $10^{-10} \text{ cm}^3/\text{s}$ , observed in [6, 8, 15], might have been due to anisotropy in the dispersion forces at short inter-atomic separations. This anisotropy is also induced by the nonzero  $L$ . We study this new mechanism of spin-exchange for the submerged-shell atom with the largest magnetic moment, dysprosium. It has an unfilled  $4f^{10}$  shell lying beneath a filled  $6s^2$  shell leading to a large orbital,  $L = 6$ , and total,  $j = 8$ , angular momentum. Its ground  $^5\text{I}_8$  state has a magnetic moment of  $\mu = 10\mu_B$ , where  $\mu_B$  is the Bohr magneton. Only recently, the first laser cooling and trapping experiments of a large number of dysprosium atoms have been reported [15]. The first measurements of inelastic collisional rates in this study suggest that anisotropy in the inter-atomic forces plays a significant role.

The paper is organized as follows. We first analyze the isotropic and anisotropic dispersion interaction between two Dy atoms in Section II and compare it with the magnetic dipole-dipole and electrostatic quadrupole-quadrupole interactions. The dispersion coefficients are calculated from atomic transition frequencies and dipole moments. The quadrupole moment of Dy is determined from a multi-configuration electronic structure calculation. In Section III we study the relative strength of the interactions in the presence of an external magnetic field and rotation. In Section IV we use these interactions to find the first estimates of the spin-exchange loss rates and compare with experimental results.

\*Corresponding author: skotoch@temple.edu

†Alternative address: St. Petersburg Nuclear Physics Institute, Gatchina, 188300; Department of Physics, St.Petersburg State University, 198904, Russia

## II. RELATIVE STRENGTH OF INTERACTION FORCES BETWEEN GROUND STATE DY ATOMS

The theoretical calculation of the ground state  $\text{Dy}_2$  potentials and their dispersion parameters is challenging due to the complexity of the spin structure of the ground-state  ${}^5\text{I}_8$  Dy atom. For example, there are 81 gerade and 72 ungerade potentials that dissociate to the  ${}^5\text{I}_8 + {}^5\text{I}_8$  limit. In spite of this complexity we have begun to calculate the van der Waals  $C_6$  coefficients for two interacting Dy atoms.

For two colliding atoms we can define the angular momentum  $\vec{J} = \vec{j}_1 + \vec{j}_2$ , its projection  $M$  along the direction of the external magnetic field  $\vec{B}$ , and its projection  $\Omega$  along the internuclear axis. For this relativistic molecule the adiabatic Born-Oppenheimer (BO) potentials are labeled by  $\Omega_\sigma^\pm$ , where  $\sigma = g/u$  for gerade and ungerade states, respectively. Gerade (ungerade) symmetry corresponds to superpositions of even (odd) values of  $J$ . The superscript  $\pm$  is only relevant for  $\Omega = 0$  states. For each  $\Omega$  there are  $17 - |\Omega|$  adiabatic Born-Oppenheimer (BO) potentials combined.

### A. Electrostatic dispersion interaction

We describe the dispersion interaction potential for two ground-state atoms in state  $|j_1 m_1, j_2 m_2\rangle$  using degenerate second-order perturbation theory similar to that given by Ref. [16]. The magnetic quantum numbers  $m_1$  and  $m_2$  are projections along the internuclear axis of the total atomic angular momenta  $\vec{j}_1$  and  $\vec{j}_2$  for the two atoms, respectively. Here  $j_1 = j_2 = 8$ . (In this section we break with convention and use roman symbols for atomic projection quantum numbers on the internuclear axis.) Matrix elements of the dispersion potentials are

$$\begin{aligned} \langle j_1 m_1, j_2 m_2 | U_{\text{disp}} | j_1 m'_1, j_2 m'_2 \rangle &= -\frac{C_6(m_1 m_2, m'_1 m'_2)}{R^6} \\ &= \sum_{\substack{n_a j_a m_a \\ n_b j_b m_b}} \frac{1}{(E_1 + E_2) - (E_{n_a j_a} + E_{n_b j_b})} \quad (1) \\ &\quad \langle j_1 m_1, j_2 m_2 | \hat{V}_{dd} | n_a j_a m_a, n_b j_b m_b \rangle \\ &\quad \times \langle n_a j_a m_a, n_b j_b m_b | \hat{V}_{dd} | j_1 m'_1, j_2 m'_2 \rangle, \end{aligned}$$

where the  $C_6(m_1 m_2, m'_1 m'_2)$  form a matrix of dispersion coefficients,  $R$  is the separation between the atoms, the sums are over all electronic states  $|n_a j_a m_a, n_b j_b m_b\rangle$  of atoms  $a$  and  $b$  excluding states with energies  $E_{n_a j_a}$  and  $E_{n_b j_b}$  equal to the ground state energies  $E_1$  and  $E_2$ . The operator  $\hat{V}_{dd}$  is the dipole-dipole interaction Hamiltonian [16]

$$\hat{V}_{dd}(\vec{R}) = \frac{1}{4\pi\epsilon_0} \frac{(\vec{d}_1 \cdot \vec{d}_2) - 3d_{1z}d_{2z}}{R^3} \quad (2)$$

where  $\epsilon_0$  is the electric constant,  $\vec{d}_1$  and  $\vec{d}_2$  are the electric dipole operators for the two atoms, and  $d_{1z}$  and  $d_{2z}$  are their components along the internuclear axis.

Using the Wigner-Eckart theorem we write the matrix  $C_6$  as

$$C_6(m_1 m_2, m'_1 m'_2) = \sum_{j_a j_b} K_{j_a j_b}^{j_1 j_2} A_{m_1 m_2, m'_1 m'_2}^{j_1 j_2 j_a j_b}, \quad (3)$$

where

$$\begin{aligned} A_{m_1 m_2, m'_1 m'_2}^{j_1 j_2 j_a j_b} &= \sum_{m_a, m_b} (1 + \delta_{m_1, m_a})(1 + \delta_{m'_1, m_a}) \\ &\quad \left( \begin{array}{ccc} j_1 & 1 & j_a \\ -m_1 & (m_1 - m_a) & m_a \end{array} \right) \left( \begin{array}{ccc} j_2 & 1 & j_b \\ -m_2 & (m_2 - m_b) & m_b \end{array} \right) \\ &\quad \left( \begin{array}{ccc} j_a & 1 & j_1 \\ -m_a & (m_a - m'_1) & m'_1 \end{array} \right) \left( \begin{array}{ccc} j_b & 1 & j_2 \\ -m_b & (m_b - m'_2) & m'_2 \end{array} \right), \end{aligned}$$

and

$$K_{j_a j_b}^{j_1 j_2} = \left( \frac{1}{4\pi\epsilon_0} \right)^2 \sum_{n_a, n_b} \frac{|\langle j_1 | d_1 | n_a j_a \rangle \langle j_2 | d_2 | n_b j_b \rangle|^2}{(E_{n_a j_a} + E_{n_b j_b}) - (E_1 + E_2)}.$$

Note that the  $A_{m_1 m_2, m'_1 m'_2}^{j_1 j_2 j_a j_b}$  conserve the molecular projection  $\Omega = m_1 + m_2 = m'_1 + m'_2$  and are independent on atomic transition frequencies and dipole moments. For this homonuclear molecule gerade/ungerade symmetry states are most conveniently constructed by transforming to states of total  $\vec{J}$ . That is to states  $|(j_1 j_2) J \Omega\rangle$  and noting that even(odd)  $J$  states have gerade(ungerade) symmetry.

There are six independent  $K_{j_a j_b}^{j_1 j_2}$  for two Dy  ${}^5\text{I}_8$  atoms as the selection rules of the electric dipole operator requires that  $|j_1 - 1| \leq j_a \leq j_1 + 1$  and  $|j_2 - 1| \leq j_b \leq j_2 + 1$ . For homonuclear dimers the  $K_{j_a j_b}^{j_1 j_2}$  is symmetric under interchange of  $j_a$  and  $j_b$ . We have determined  $K_{j_a j_b}^{j_1 j_2}$  using 62 experimental transition frequencies and oscillator strengths from the ground to various excited states of the Dy atom [17]. Table I lists the values of  $K_{j_a j_b}^{j_1 j_2}$ .

The adiabatic dispersion potentials and, thus, the long-range of the Born-Oppenheimer potentials are found by the diagonalizing the  $C_6$  matrices for each  $\Omega_{g/u}^\pm$ . Figure 1 shows the adiabatic gerade and ungerade  $C_6$  coefficients as a function of the projection quantum number  $\Omega$  of the total angular momentum  $J$  on the interatomic axis. The number of adiabatic  $C_6$  values is smaller for larger  $\Omega$ . In fact, for  $\Omega = 16$  there is only one potential. It has gerade symmetry. In total there are 81/72 dispersion coefficients corresponding to the ground state gerade/ungerade potentials. The coefficients in Fig. 1 show a smooth nearly parabolic behavior with the projection number  $\Omega$ . This  $\Omega$  dependence is a consequence of the anisotropic coupling of the open  $f$ -shell electrons of the two atoms. As a result the interaction energy depends on the relative orientation of the atoms.

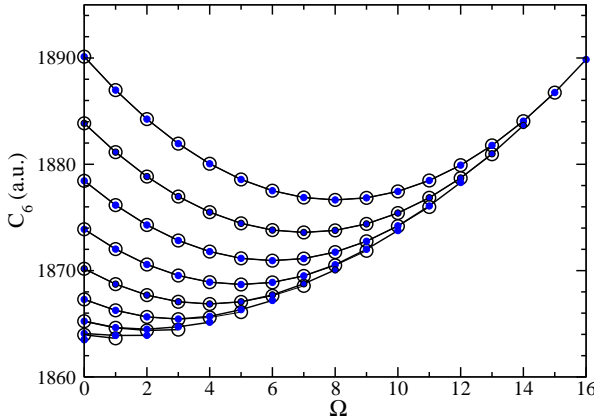


FIG. 1: Gerade (filled circles) and ungerade (open circles) adiabatic  $C_6$  coefficients for the interaction between two ground  $^5I_{j=8}$  state Dy atoms as a function of the projection  $\Omega$  of the total angular momentum  $\vec{J}$  on the interatomic axis. The difference between the dispersion coefficients for the gerade/ungerade symmetry is small and invisible on the graph. A larger  $C_6$  coefficient implies a deeper Born-Oppenheimer potential.

### B. Magnetic dipole-dipole and electrostatic quadrupole-quadrupole interaction

The matrix elements of the magnetic dipole-dipole interaction between two magnetic dipoles  $\vec{\mu} = g_j \mu_B \vec{j}$  is

$$\langle j_1 m_1, j_2 m_2 | U_{\text{mdd}} | j_1 m'_1, j_2 m'_2 \rangle = -\frac{C_3(m_1 m_2, m'_1 m'_2)}{R^3} = \langle j_1 m_1, j_2 m_2 | \hat{V}_{\mu\mu} | j_1 m'_1, j_2 m'_2 \rangle, \quad (4)$$

where  $\hat{V}_{\mu\mu}$  is magnetic dipole-dipole operator

$$\hat{V}_{\mu\mu} = \frac{\mu_0 (g_j \mu_B)^2}{4\pi} \frac{(\vec{j}_1 \cdot \vec{j}_2) - 3j_{1z}j_{2z}}{R^3}, \quad (5)$$

and  $g_j = 1.24159$  is the g-factor for the ground  $^5I_8$  state of the Dy atom [18], and  $\mu_0$  is the magnetic constant. A more accurate value for the magnetic moment of Dy is  $\mu = g_j \mu_B \times j = 9.93 \mu_B$ .

Figure 2 shows the adiabatic gerade and ungerade  $C_3$  coefficients as a function of  $\Omega$ . These coefficients are obtained by diagonalizing the matrix Eq.(4) at each  $R$ . The

TABLE I: The  $K_{j_a j_b}^{j_1 j_2}$  matrix elements in atomic units for the dipole transitions from  $j_1 = j_2 = 8$  to  $j_a, j_b = 7, 8$ , or 9 for two interacting Dy atoms.

$j_a/j_b$	7	8	9
7	71528.597	81313.663	88173.833
8	81313.662	92438.922	100240.311
9	88173.833	100240.311	108705.654

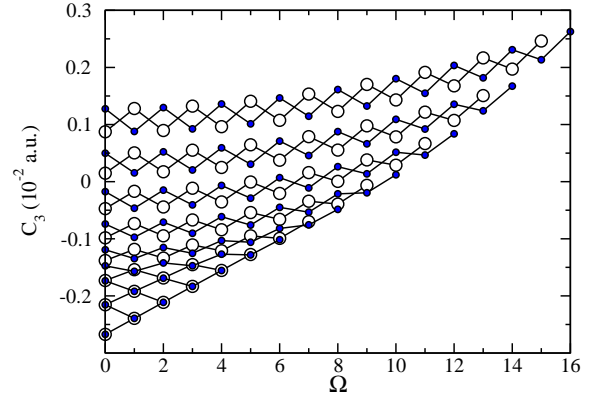


FIG. 2: Gerade (filled circles) and ungerade (open circles) adiabatic  $C_3$  coefficients for the interaction between two ground  $^5I_{j=8}$  state Dy atoms as a function of the projection  $\Omega$  of the total angular momentum  $\vec{J}$  on the interatomic axis. A larger  $C_3$  coefficient implies a deeper Born-Oppenheimer potential.

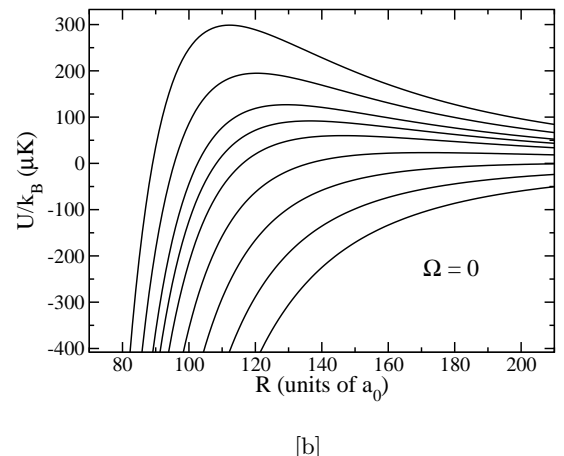


FIG. 3: Adiabatic gerade interaction potentials of the combined electrostatic dispersion and magnetic dipole-dipole forces between two Dy atoms in the ground  $^5I_8$  state and projection  $\Omega=0$ . Here  $k_B$  is the Boltzmann constant. The effect of rotation is not included.

values are both positive and negative. A comparison with the adiabatic  $C_6$  coefficients in Fig. 1 shows a different  $\Omega$  dependence.

A more accurate description of the long-range interaction is obtained by first adding the dispersion  $U_{\text{disp}}$  and magnetic dipole-dipole  $U_{\text{mdd}}$  interactions together and diagonalize at each internuclear separation  $R$ . Unlike, for the previous cases the eigenfunctions now depend on  $R$ . As an example, the resulting adiabatic gerade potentials for projection  $\Omega=0$  as a function of  $R$  are shown in Fig. 3. At small  $R$  the dispersion interaction dominates,

whereas for  $R > 150 a_0$  the magnetic dipole-dipole interaction plays a major role. For intermediate  $R$  these forces compete leading to both attractive and repulsive potentials depending on sign of the  $C_3$  coefficient.

Our unrestricted coupled cluster calculation with single, double, and perturbative triple excitations UCCSD(T) [19] shows that the quadrupole moment of the Dy atom in the  $^5\text{I}_8$  state is very small and equal to  $Q=-0.00524$  a.u.. As a result the quadrupole-quadrupole interaction energy is seven orders of magnitude weaker than the other atom-atom interactions.

### III. INTERACTIONS IN A MAGNETIC TRAP

We now analyze the relative strength of all interactions between two Dy atoms in a magnetic field. The magnetic field is added as either the atoms are held in a magnetic trap [15] with a spatially varying field strength or are held in an optical trap with an homogeneous  $B$  field to control the interaction between the atoms. In addition, the molecule can rotate, which is described by the Hamiltonian  $\hbar^2 \vec{\ell}^2 / (2m_r R^2)$ , where  $\vec{\ell}$  is the relative orbital angular momentum between the two atoms and  $m_r$  is the reduced mass.

It is convenient to choose a coordinate system with projection quantum numbers defined along the external magnetic field direction. Again following convention, projection quantum numbers are labeled by roman symbols. In this coordinate system the rotational and Zeeman interactions as well as the isotropic or “average” dispersion potential shift molecular levels, whereas the magnetic dipole-dipole interaction and anisotropic component of the dispersion potential lead to coupling between different rotational and Zeeman components. As a result, the angular momentum projection  $M$  of  $\vec{J}$  can change up to 2 units due to the magnetic dipole interaction and up to 4 units due to the anisotropic dispersion potential [20].

Figure 4 shows various anisotropic properties that can lead to reorientation of the Dy angular momenta as a function of  $R$ . Firstly, the Zeeman splitting  $g_j \mu_B B$  between neighboring magnetic sublevels for magnetic field strength of 10 and 100 Gauss are shown. The anisotropic potential  $\Delta C_6 / R^6$  is drawn assuming a typical value of  $\Delta C_6 = 25$  a.u., based on the spread of  $C_6$  value shown in Fig. 1. We also present the splitting between the rotational levels  $\ell=0$  and 2 of the ground state as  $6\hbar^2 / (2m_r R^2)$ . Finally, the value of splitting due to magnetic dipole-dipole interaction is given.

For different interatomic separations different forces dominate. In fact, when the curves for the magnetic dipole or anisotropic dispersion interaction cross the Zeeman or rotational energies spin flips can occur. At large  $R$  the Zeeman splitting is dominates. Both magnetic dipole-dipole and anisotropic electrostatic curves cross the Zeeman  $B = 100$  G curve at  $R < 35a_0$ , where chemical bonding should play an important role as well. For the weaker magnetic field of  $B = 10$  G the spin coupling

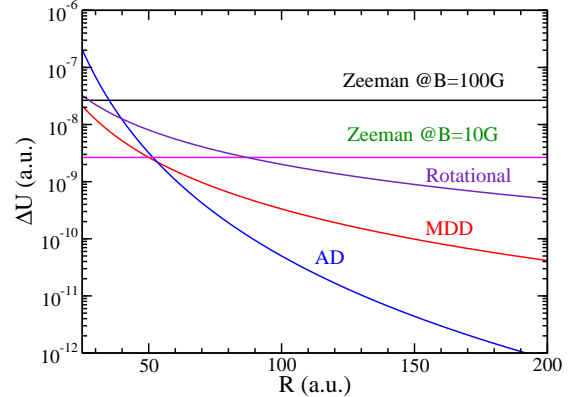


FIG. 4: Level splitting due to the dominant interaction forces in atomic units as a function of interatomic separation. In atomic units the Zeeman splitting is  $g_j B / 2$ , the splitting between  $\ell=0$  and 2 rotational levels is given by  $6 / (2m_r R^2)$ , the splitting due to the magnetic dipole-dipole (MDD) interaction is  $2\alpha^2 j(g_j/2)^2 / R^3$ , where  $\alpha$  is the fine structure constant, and the anisotropic dispersion (AD) interaction is  $\Delta C_6 / R^6$ , where  $\Delta C_6 = 25$  a.u.. Here  $m_r$  is the reduced mass in units of the electron mass.

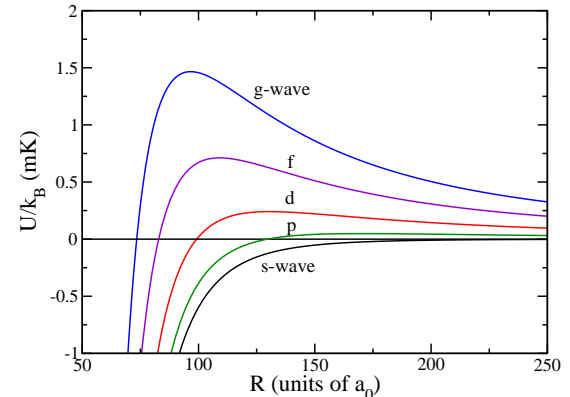


FIG. 5: Dispersion interaction potentials for  $C_6 = 1890$  a.u. for the lowest five partial waves with centrifugal barriers for  $p$ -,  $d$ -,  $f$ -, and  $g$ -waves

occurs for  $R$  near  $50a_0$ . The interactions will lead to mixing of rotational levels for  $R < 50a_0$  as well.

### IV. FIRST ESTIMATE OF INELASTIC RATE COEFFICIENTS

In this paper we complete our analysis of the interaction between ultracold  $^{164}\text{Dy}$  atoms by a first estimate of inelastic loss rates due to the anisotropy in the dis-

persion and magnetic dipole-dipole interaction. We will perform a separate estimate of losses from these interactions. For both cases we consider atoms in a magnetic field with a strength of the order of 1 G as described in the recent experiment [15], with the goal to model its losses. The experiment started from a gas of Dy atoms in a quadrupole magnetic trap with atoms distributed over atomic magnetic sublevels with positive magnetic moment. Ie. states  $|jm\rangle$  with  $m > 0$  where the projection  $m$  is defined along the magnetic field direction. Inelastic spin-exchange collisions to states with  $m \leq 0$  lead to atom loss.

We first describe a model for the loss due to the anisotropic dispersion potentials based on an universal single-channel scattering model developed and used in Refs. [21–23]. This universal loss model assumes scattering from a single potential of the form  $-C_6/R^6 + \hbar^2\ell(\ell+1)/(2m_rR^2)$  for  $R > R_c$  and that all flux that reaches the critical separation  $R_c$  undergoes irreversible spin-exchange independent of collision energy and partial wave  $\ell$ .

For Dy we can use this universal model under several assumptions. We first note that the anisotropy  $\Delta C_6$  of the dispersion potential is small compared to the average or isotropic dispersion potential. Secondly, an external magnetic field is applied that splits the different  $m$  levels and, as shown in Fig. 4, the spin flip occurs between  $R_c = 35a_0$  and  $50a_0$  depending on the magnetic field strength. We can therefore apply the universal model assuming a mean isotropic  $C_6$  value and that, due to the anisotropic dispersion potential, no flux returns from  $R < R_c$ .

For temperatures between 100  $\mu\text{K}$  to 1 mK only a few partial waves  $\ell$  contribute to the collisions. Figure 5 illustrates this by showing the centrifugal barriers for  $s, p, d$ , and  $f$  and  $g$  partial waves as a function of  $R$ . The temperature range of interest lies well below the  $g$ -wave barrier. Within the universal scattering model the contribution to the inelastic rate coefficient for partial wave  $\ell$  and projection  $m_\ell$  is

$$K_{\ell m_\ell}(E) = v_i \frac{\pi}{k_i^2} (1 - |S_{\ell m_\ell}(E)|^2), \quad (6)$$

where  $E = k_i^2/(2m_r)$  is the collision energy,  $k_i$  is the initial relative wavenumber,  $v_i$  is the initial relative velocity, and the  $S_{\ell m_\ell}(E)$  are diagonal scattering  $S$ -matrix elements. The solution  $\Psi_{\ell m_\ell}(R)$  of the radial Schrödinger equation for the single-channel potential with boundary condition

$$\Psi_{\ell m_\ell}(R) \propto e^{-i(R_x/R)^2/2}$$

at short range  $R < R_c$  with  $R_x = \sqrt{2m_r C_6/\hbar^2}$  and

$$\Psi_{\ell m_\ell}(R) = \frac{e^{-ik_i R}}{\sqrt{k_i}} - S_{\ell m_\ell}(E) \frac{e^{ik_i R}}{\sqrt{k_i}}$$

at large  $R$  determines the  $S_{\ell m_\ell}$  matrix elements. The partial and total loss rate coefficient are  $\beta_\ell(E) =$

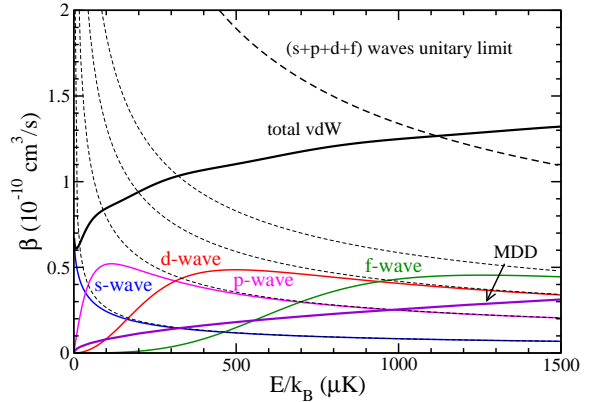


FIG. 6: The inelastic loss rate coefficient for a non-spin-polarized sample of ground state  $^{164}\text{Dy}$  atoms as a function of collision energy based on an universal scattering model for losses due to the anisotropy of the dispersion potential and a Born approximation for losses from the magnetic dipole-dipole interaction. For the universal scattering model rate coefficients for the lowest four partial waves as well as summed rate are shown. The loss rate coefficient for the magnetic dipole-dipole interaction is indicated by the abbreviation MDD. The unitary limited loss rate coefficients for the lowest four partial waves are plotted as dashed lines.

$2 \sum_{m_\ell} K_{\ell m_\ell}(E)$  and  $\beta(E) = 2 \sum_{m_\ell} K_{\ell m_\ell}(E)$ , respectively. The factor of 2 is due to the fact that after each collision two atoms are lost. Partial and total inelastic loss rate coefficients are shown in Fig. 6 for collision energies up to 1.5 mK. The figure shows that the loss rate for the different partial waves becomes large for collision energies approaching the corresponding centrifugal barrier. Moreover, except for extremely small collision energies the total loss rate coefficient slowly increases with energy. For comparison we have also indicated the unitarity limit for each partial wave. The unitarity occurs when  $|S_{\ell m_\ell}(E)|^2 = 0$  for all collision energies.

We now turn to a model for losses due to spin exchange induced by the magnetic dipole-dipole interaction. For simplicity we assume that the atoms are in the stretched state with  $m = +j$ . We estimate this inelastic loss rates using first-order perturbation theory similar to that applied for the calculation of the dipolar relaxation rates in a gas of chromium atoms [1]. We immediately note that the magnetic moment of dysprosium or chromium atoms is large and, therefore, a perturbative theory may not provide an accurate loss rates. However, it is expected to give a reasonable estimate. Following Ref. [1], the loss rate coefficient for a single spin flip with  $M \rightarrow M - 1$  (i.e. from  $M=16$  to  $15$ ), averaged over all possible relative orientations of the initial relative momentum  $\vec{k}_i$ , is

$$\gamma_1 = \frac{4\pi}{15} j^3 \left( \frac{\mu_0(g_j\mu_B)^2\mu_r}{2\pi\hbar^2} \right)^2 [1 + h(k_f/k_i)] \frac{\hbar k_f}{\mu_r}, \quad (7)$$

where  $\hbar^2 k_f^2 / (2\mu_r) = g_j \mu_B B$  and

$$h(x) = -1/2 - (3/4)(1-x^2)^2 \log[(x-1)/(x+1)]/(x(1+x^2))$$

for  $x > 1$ .

Similarly, for a double spin flip with  $M \rightarrow M - 2$  the rate coefficient is

$$\gamma_2 = \frac{2\pi}{15} j^2 \left( \frac{\mu_0 (g_j \mu_B)^2 \mu_r}{2\pi \hbar^2} \right)^2 [1 + h(k_f/k_i)] \frac{\hbar k_f}{\mu_r}, \quad (8)$$

where now  $\hbar^2 k_f^2 / (2\mu_r) = 2g_j \mu_B B$ . The total dipole-dipole loss rate is given by  $\gamma = 2(\gamma_1 + \gamma_2)$  and shown as a function of collision energy in Fig. 6.

The loss rates in Fig. 6 are smaller than the rate measured in Ref. [15] as  $2.1(2) \times 10^{-10} \text{ cm}^3/\text{s}$  for temperatures around  $500 \mu\text{K}$ . This suggests the presence of a resonance in the scattering process. In fact, flux of atoms can return from small  $R$ , interfere with the incoming flux to lead to an increasing loss. We obtained a similar effect in our analysis of the reactive collisions between two KRb molecules [24].

## V. CONCLUSION

In conclusion, we have studied the origin of the anisotropy in the long-range interaction between ground state dysprosium atoms. This is a first step towards a

complete multi-channel description of inelastic and elastic collision between such atoms. We find van der Waals coefficients by using known atomic dipole moments and energy levels. Our coefficients form a lower bound. We show that the splitting between or anisotropy of the Born-Oppenheimer potentials is almost two order of magnitude smaller than their average or isotropic potential. In addition, we have presented two approximate single-channel calculations to estimate inelastic losses when Dy atoms are not in the energetically-lowest Zeeman sublevel. The first model describes losses due to the anisotropy of the dispersion potentials and is based on an universal scattering theory. The second perturbative model describes losses due to the magnetic dipole-dipole interaction. The only way to obtain a clear and quantitative understanding of collisions between Dy atoms is by a coupled-channel calculation. We will do so in the near future. It will enable us to predict location of magnetic Feshbach resonances in the energetically-lowest Zeeman level.

## VI. ACKNOWLEDGMENTS

This work is supported by grants of the Air Force Office of Scientific Research and NSF PHY-1005453. We acknowledge helpful discussions on the Dy electronic structure with Dr. J. Reader and stimulating discussions with Dr. B. Lev, Dr. E. Tiesinga, and Dr. J. Bohn.

---

[1] S. Hensler, J. Werner, A. Griesmaier, P. O. Schmidt, A. Görslitz, T. Pfau, S. Giovanazzi, and K. Rzazewski, *Appl. Phys. B* **77**, 765 (2003).

[2] C. I. Hancox, S. C. Doret, M. T. Hummon, L. Luo, and J. Doyle, *Nature* **431**, 281 (2004).

[3] C. I. Hancox, S. C. Doret, M. T. Hummon, R. V. Krems, and J. M. Doyle, *Phys. Rev. Lett.* **94**, 013201 (2005).

[4] R.V. Krems, J. Klos, M. F. Rode, M. M. Szczesniak, G. Chalasiński, and A. Dalgarno, *Phys. Rev. Lett.* **94**, 013202 (2005).

[5] J. Stuhler, A. Griesmaier, T. Koch, T. Pfau, S. Giovanazzi, P. Pedri, and L. Santos, *Phys. Rev. Lett.* **95**, 150406 (2005).

[6] J. G. E. Harris, S.V. Nguyen, S. C. Doret, W. Ketterle, and J. M. Doyle, *Phys. Rev. Lett.* **99**, 223201 (2007).

[7] T. Lahaye, T. Koch, B. Fröhlich, M. Fattori, J. Menz, A. Griesmaier, S. Giovanazzi, and T. Pfau, *Nature* **448**, 672 (2007).

[8] C. B. Connolly, Y. Shan Au, S. C. Doret, W. Ketterle, and J. M. Doyle, *Phys. Rev. A* **81**, 01000702(R) (2010).

[9] B. Fregoso and E. Fradkin, *Phys. Rev. Lett.* **103**, 205301 (2009); B. Fregoso and E. Fradkin, *Phys. Rev. B* **81**, 214443 (2010).

[10] R. Wilson, S. Ronen, and J. Bohn, *Phys. Rev. A* **80**, 023614 (2009).

[11] M. A. Baranov, A. Micheli, S. Ronen, and P. Zoller, *Phys. Rev. A* **83**, 043602 (2011).

[12] Daw-Wei Wang, Mikhail D. Lukin, and Eugene Demler, *Phys. Rev. Lett.* **97**, 180413 (2006).

[13] M. Lewenstein, *Nature Phys.* **2** 2 (2006).

[14] E. B. Aleksandrov *et al.*, *Opt. Spectrosc.* **54**, 1 (1983).

[15] M. Lu, S. Ho Youn, and B. Lev, *Phys. Rev. Lett.* **104**, 063001 (2010).

[16] A. J. Stone, *The theory of intermolecular forces*, (Clarendon Press, London, 1996).

[17] M. E. Wickliffe, J. E. Lawler, and G. Nave, *J. Quantitative Spectroscopy & Radiative Transfer* **66**, 363-404 (2000); J. J. Curry, E. A. Den Hartog, and J. E. Lawler, *J. Opt. Soc. Am. B* **14**, 2788 (1997); V. N. Gorshkov, V. A. Komarovskii, A. L. Osherovich, N. P. Penkin, and R. Khefferlin, *Opt. Spectrosc.* **48**, 362 (1980).

[18] Ralchenko, Yu., Kramida, A.E., Reader, J., and NIST ASD Team (2010). NIST Atomic Spectra Database (ver. 4.0.1), <http://physics.nist.gov/asd>

[19] J. D. Watts, J. Gauss, and R. J. Bartlett, *J. Chem. Phys.* **98**, 8718 (1993).

[20] R. Santra and C. H. Greene, *Phys. Rev. A* **67**, 062713 (2003).

[21] P. S. Julienne and F. H. Mies, *J. Opt. Soc. Am. B* **6**, 2257 (1989).

[22] C. Orzel, M. Walhout, U. Sterr, P. S. Julienne, and S. L. Rolston, *Phys. Rev. A* **59**, 1926 (1999).

[23] E. R. Hudson, N. B. Gilfoy, S. Kotochigova, J. M. Sage, and D. DeMille, *Phys. Rev. Letter* **100**, 203201 (2008).

[24] S. Kotochigova, *New J. Phys.* **12**, 073041 (2010).